

The effect of damping on a simulation for the dispersion curve of the surface wave

Zan Zhou¹, and Thomas M.H. Lok²

¹ Department of Civil and Environmental Engineering, University of Macau, Macau SAR, China

² Department of Civil and Environmental Engineering, University of Macau, Macau SAR, China

E-mail: yb87457@connect.um.edu.mo

ABSTRACT: Over the past two decades, noninvasive tests have attained a lot of attention to infer soil properties, especially, the surface wave method. However, whether some soil properties, such as the damping ratio of the soil, affect significantly the propagation of surface wave has not been answered. In this study, a series of numerical tests are carried out using the finite element method to investigate the effect of damping on the displacement on the ground surface and the dispersion curve of surface waves. The analytical results show that by considering the damping ratio of soil, the reflection from the boundary of the finite element model can be decreased effectively. With increasing damping, the reflection gradually decreases and eventually disappears. When the reflection disappears, the resolution of the extracted dispersion curve can be improved correspondingly. The resolution of the dispersion curve can influence the inversion results, so improving the resolution is meaningful.

KEYWORDS: Surface wave, dispersive curve, damping, finite element method.

1. INTRODUCTION

Over the past two decades, noninvasive tests have attained a lot of attention to infer soil properties. Compared with invasive tests, noninvasive tests are environmentally friendly. Especially, the surface wave methods which can be used to determine the shear wave velocity profile of the subsurface, compared to other feasible methods, are much cheaper (Olafsdottir et al. 2018).

Currently, the surface wave methods can be divided into two kinds, one is the spectral analysis of surface waves (SASW) (Heisey et al. 1982, Gucunski and Woods 1992), and the other is the multichannel analysis of surface waves (MASW) (Park et al. 1999, Xia et al. 1999). The MASW is a newer and more robust technique, which overcomes some weaknesses of SASW (Park et al. 1999, Olafsdottir et al. 2018). The surface wave methods are divided into three steps: Field measurements, dispersion analysis, and inversion analysis (Ólafsdóttir 2019). In the past, most researchers paid attention to the third step, and a lot of inversion methods were proposed. Xia et al. (1999) used the Levenberg—Marquardt and singular-value decomposition techniques to infer the shear wave velocity profile. Wathelet et al. (2004) adopted a direct search algorithm to carry out the inversion analysis. Ryden and Park (2006) utilized the fast simulated annealing algorithm to conduct the inversion analysis. Song et al. (2015) applied an artificial bee colony algorithm on surface wave inversion. However, there is still a lack of sufficient understanding of the relationship between soil properties and surface wave dispersion curves. Because the subsurface condition is like a black box, it is hard to study the relationship directly by the surface wave methods. If the subsurface condition can be known exactly, it is meaningful to perform a surface wave test and investigate the relationship between soil properties and surface wave dispersion curves. Gucunski and Woods (1992) used a numerical method to simulate the SASW test. Roy and Jakka (2017) simulated the MASW test by FEM and study the near-field effects of the surface wave. In the application of the surface wave method, the quality of the dispersion curve affects the final inversion results. In the entire inversion analysis process, by continuously adjusting the shear wave velocity profile, the error between the calculated dispersion curve and the observed dispersion curve is as small as possible. A lot of methods can be used to calculate the theoretical dispersion curve, such as the transfer matrix method (Thomson 1950, Haskell 1953, Nazarian 1984), global matrix method (Nazarian 1984, Lowe 1995), stiffness matrix method (Kausel and Roësset 1981, Gucunski and Woods 1992, Ganji et al. 1998), and so on. However, in the above calculation process, the soil damping is ignored. In the real case, damping is a basic property of soil. Therefore, studying the effect of the damping ratio on the dispersion curve is necessary.

In this study, a numerical model with two different soil layers is built and a MASW test is simulated, from which the vertical displacement on the ground surface can be recorded. The different dispersion curves can be obtained by the phase shift method (Park et al. 1998). The following study will investigate the effects of the material damping of soil on the resolution of the extracted dispersion curve.

2. METHODOLOGY

2.1 MASW test simulation

A typical MASW test, as shown in Figure 1, usually includes 24 receivers. The test procedure:

- Using a hammer to hit the ground to produce seismic waves.
- When the seismic waves arrive at the different receivers, the signal will be recorded by these receivers.
- The signal will be output to a PC and stored for further analysis.

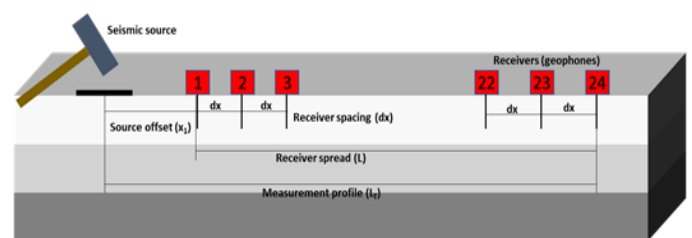


Figure 1 Typical MASW measurement profiles with 24 receivers

These seismic waves are produced by a hammer, so the seismic source can be assumed as a vertical point source, and wave propagation follows a cylindrical spread centered on the seismic source, as shown in Figure 2. However, the current analytical methods adopt the plain strain assumption. In addition, Roy and Jakka (2017) performed some numerical tests to study the near-field effect. Current research results show that as long as the source offset is large enough, the near-field effect can be ignored. Therefore, this study used an axisymmetrical model to simplify the numerical analysis.

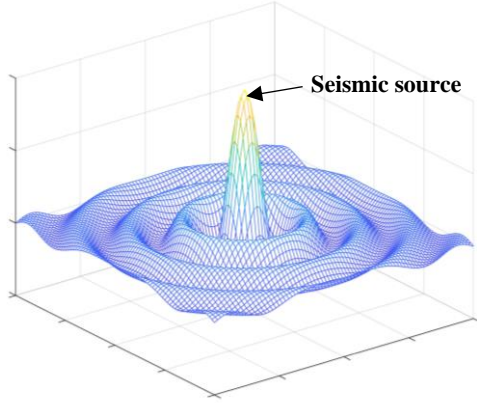


Figure 2 2D radiation pattern of Rayleigh surface waves generated by a vertical point source

When the hammer hits the ground surface, seismic waves will be produced. The governing equation for a system subjected to a dynamic loading $F(t)$ can be described as follows:

$$M\ddot{u}(t) + C\dot{u}(t) + Ku(t) = F(t) \quad (1)$$

Where M , C , and K are the $N \times N$ mass, damping, and stiffness matrix. $\ddot{u}(t)$, $\dot{u}(t)$ and $u(t)$ are acceleration, velocity, and displacement vectors.

Due to the nature of the dynamic loading, solving Eq. (1) becomes quite complex. Therefore, numerical methods are fairly efficient ways to find approximate solutions to this equation, especially the finite element method (FEM). In this study, PLAXIS (PLAXIS (2023)) was used to model the MASW test.

Eq. (1) can be solved by implicit time integration schemes such as the Newmark method. The C in Eq. (1) accounts for the material damping in materials. Material damping occurs due to friction or irreversible deformations such as plasticity or viscosity. The more viscous or plastic the material, the more energy can be dissipated. Even when elasticity is assumed, damping can be considered using the C . However, determining the damping matrix requires additional parameters that are difficult to obtain from tests. In finite element formulations, C is often expressed as a function of the mass and stiffness matrices, known as Rayleigh damping.

$$C = \alpha_R M + \beta_R K \quad (5)$$

Where the α_R and β_R represent the Rayleigh coefficients.

In addition, in order to suppress the reflections of waves in the model boundary, special absorbent boundaries are imposed at the boundary.

The viscous boundaries implemented in the PLAXIS are introduced. These boundaries are based on the Lysmer-Kohlmeyer model (Lysmer and Kuhlemeyer 1969). According to this model, a damper absorbs the components of normal and shear stress, as described by the equations below.

$$\sigma_n = -C_1 \rho V_p \dot{u}_x \quad (6)$$

$$\tau = -C_2 \rho V_s \dot{u}_y \quad (7)$$

Where ρ is the density, V_s is the shear wave velocity, and V_p is the compressive wave velocity. The velocity of particle motion in the x direction is represented by \dot{u}_x , while \dot{u}_y represents the velocity in the y direction. C_1 and C_2 are relaxation coefficients that are used to

improve boundary absorption. In this study, these two values adopt the default values of 1.0.

2.2 FEM Model Verification

When the hammer hits the ground surface, an impulse loading will be produced, and this loading is simulated using a half-sine pulse over a short duration. The load peaks at 12 kN and lasts for 0.012 seconds. The simulation runs for a total of 1 second with a time step of 0.001 seconds, as shown in the following figure.

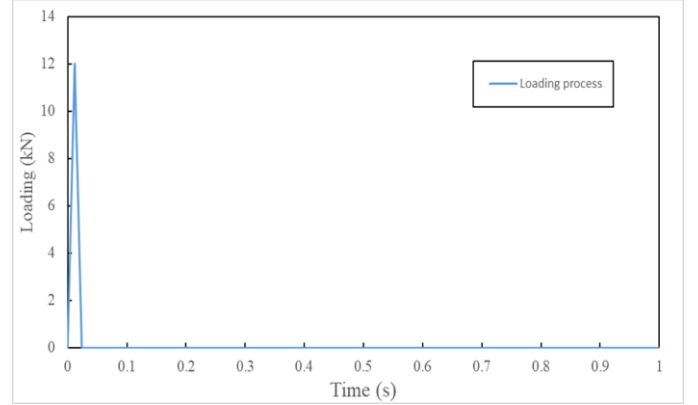


Figure 3 Simulated impulse loading

The entire FEM model is shown in Figure 4. This axisymmetric model with a 200m in radius and 300m in height. The impulse loading is applied at the center of the model. In addition, the 24 receivers are distributed evenly over the ground with a distance of one meter, and the first receiver is 10m away from the impulse loading. The left, right, and bottom of the model are modeled by the viscous boundaries, and the top is a free boundary. There are 1458 elements in total, and all elements are triangle elements with 15 nodes. Furthermore, the mesh density in the area of receivers and impulse loading are refined to produce enough points to record the vertical displacement.

In this FEM model, there are two different kinds of soils, and the thickness of the top layer of soil is 10m. For these two kinds of soils, the corresponding material parameters are shown in Table 1.

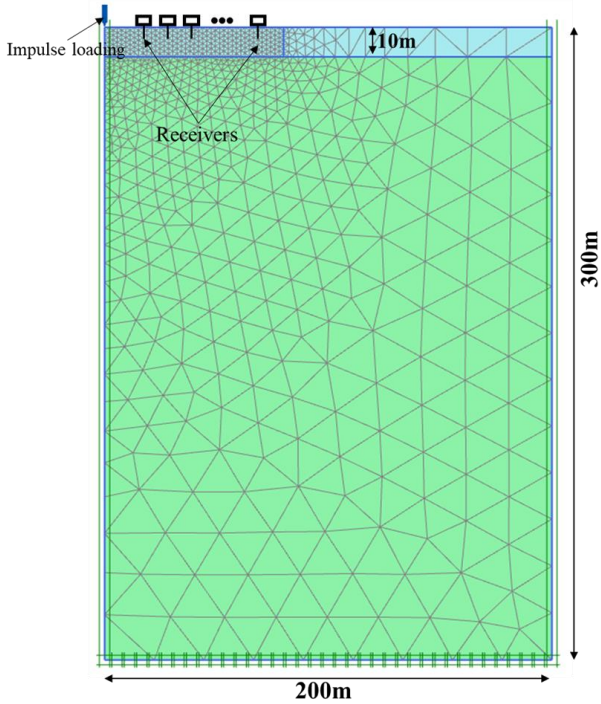


Figure 4 FEM model of MASW test

Table 1 The material parameters of the verification case

Parameters	Upper soil	Lower soil
Density (ρ)	1.8kg/m ³	1.8kg/m ³
Poisson's Ratio (μ)	0.3	0.3
Shear wave velocity (V_s)	180m/s	300m/s
Compressive wave velocity (V_p)	336.7m/s	561.2m/s
α_R	0	0
β_R	0	0

The detailed verification results are provided in Figure 5. Based on Figure 5 (c), the error between theoretical and experimental results is relatively small and about 1.8346%, which means this verification is accurate enough. However, there are still some problems, for example, in Figure 5(a), there are still large reflected waves, even though the viscous boundary conditions are used. This phenomenon is also evident in Figure 5(b), which will affect the extraction of the dispersion curve from this figure. In addition, in Figure 5(c), the theoretical dispersion curve is a little off from the experimental one when the wavelength is larger than 25 m. The reason is that, in these areas, the frequency is low, and the corresponding variance of the normalized amplitude along the phase velocity is larger, which can be seen in Figure 5(b), so the deviation between the theoretical dispersion curve and the experimental one becomes larger when the wavelength is larger than 25 m.

Note: explain the meanings of legend in Fig. 5(c)

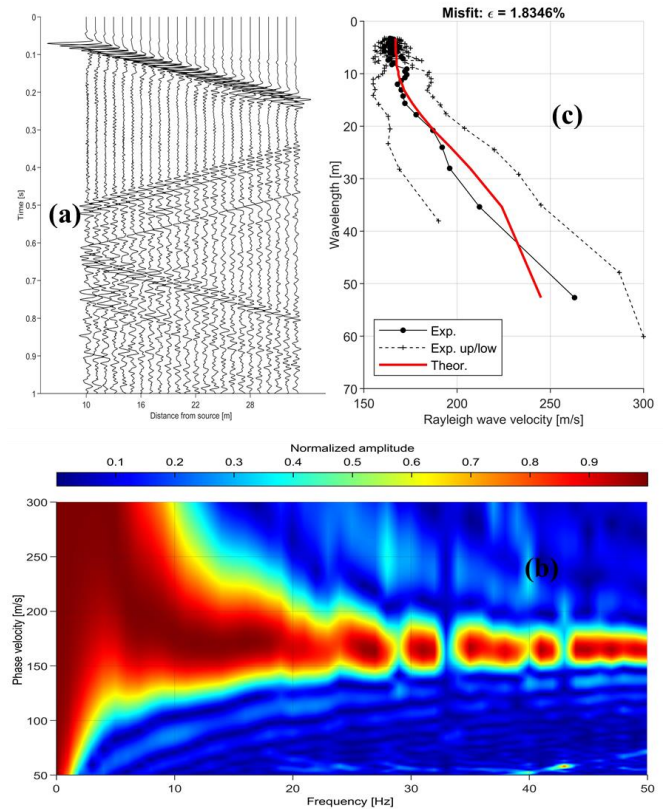


Figure 5 Results of FEM analysis (a) Vertical displacement for different 24 receivers (b) Transformation from the distance-time domain to the frequency-velocity domain (c) Comparison between theoretical and experimental results

3. RESULTS OF FEM ANALYSIS

According to the previous results, the viscous boundaries are not enough to avoid the reflections of waves. However, damping is a non-negligible parameter of soil. In past studies, researchers usually ignore this parameter.

In this study, the effect of damping on the dispersion curve is studied. The previous FEM model is used with material damping shown in Table 2, and these values are trade-offs between the reflection of waves and resolution in the frequency-phase velocity domain, while other material parameters remain at the same values.

Table 2 Updated material parameters

Parameters	Upper soil	Lower soil
α_R	1e-4	1e-4
β_R	1e-3	1e-3

With these updated parameters in the FEM model, the final results are shown in Figure 6. From Figure 6(a), the reflection of waves is almost invisible. In addition, in Figure 6(b), the area with high amplitude is gathered, which means that the extraction of the dispersion curve becomes relatively easier. Finally, by picking the peak values from Figure 6(b), the corresponding dispersion curve is obtained, as shown in Figure 6(c). The error between the theoretical and experimental dispersion curves is smaller and about 1.5603%, which means the extracted dispersion with damping can provide a more accurate dispersion curve.

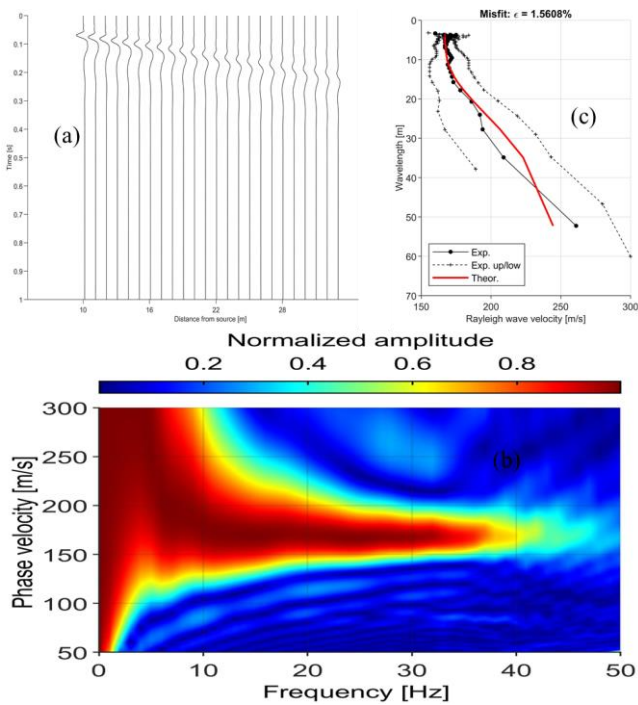


Figure 6 Results of FEM analysis with damping of soil
(a) Vertical displacement for different 24 receivers
(b) Transformation from the distance-time domain to the frequency-velocity domain
(c) Comparison between theoretical and experimental results

4. CONCLUSIONS

In this study, a FEM model was used to simulate the MASW test. Without material damping, the FEM can model the MASW test successfully. However, according to the verification, although the viscous boundaries are adopted, the reflection of waves is obvious in the model without material damping. To reduce the reflection of waves, but also to more reasonably simulate the real experimental environment, a FEM model considering the material damping of soils was adopted. With the material damping of soils, the reflection of waves decreases obviously. At the same time, the resolution of frequency and velocity contour is also improved, which makes the dispersion curve more accurate.

5. REFERENCES

Ganji, V., N. Gucunski and S. Nazarian (1998). Automated inversion procedure for spectral analysis of surface waves. *Journal of geotechnical and geoenvironmental engineering* **124**(8): 757-770.

Gucunski, N. and R. D. Woods (1992). Numerical simulation of the SASW test. *Soil Dynamics and Earthquake Engineering* **11**(4): 213-227. [https://doi.org/10.1016/0267-7261\(92\)90036-D](https://doi.org/10.1016/0267-7261(92)90036-D).

Haskell, N. A. (1953). The dispersion of surface waves on multilayered media*. *Bulletin of the Seismological Society of America* **43**(1): 17-34. 10.1785/bssa0430010017.

Heisey, J., K. Stokoe and A. Meyer (1982). Moduli of pavement systems from spectral analysis of surface waves. *Transportation research record* **852**(22-31): 147.

Kausel, E. and J. M. Roësset (1981). Stiffness matrices for layered soils. *Bulletin of the seismological Society of America* **71**(6): 1743-1761.

Lowe, M. J. S. (1995). Matrix techniques for modeling ultrasonic waves in multilayered media. *IEEE Transactions on Ultrasonics, Ferroelectrics, and Frequency Control* **42**(4): 525-542. 10.1109/58.393096.

Lysmer, J. and R. L. Kuhlemeyer (1969). Finite Dynamic Model for Infinite Media. *Journal of the Engineering Mechanics Division* **95**(4): 859-877. doi:10.1061/JMCEA3.0001144.

Nazarian, S. (1984). In situ determination of elastic moduli of soil deposits and pavement systems by spectral-analysis-of-surface-waves method, The University of Texas at Austin.

Ólafsdóttir, E. Á. (2019). Multichannel Analysis of Surface Waves for Soil Site Characterization. Ph.D., University of Iceland.

Ólafsdóttir, E. Á., S. Erlingsson and B. Bessason (2018). Tool for analysis of multichannel analysis of surface waves (MASW) field data and evaluation of shear wave velocity profiles of soils. *Canadian Geotechnical Journal* **55**(2): 217-233. 10.1139/cgj-2016-0302.

Park, C. B., R. D. Miller and J. Xia (1998). Imaging dispersion curves of surface waves on multi-channel record. SEG Technical Program Expanded Abstracts 1998, Society of Exploration Geophysicists; 1377-1380.

Park, C. B., R. D. Miller and J. Xia (1999). Multichannel analysis of surface waves. *GEOPHYSICS* **64**(3): 800-808. 10.1190/1.1444590.

PLAXIS (2023). PLAXIS 2D Reference Manual. Bentley Systems International Limited. Dublin.

Roy, N. and R. S. Jakka (2017). Near-field effects on site characterization using MASW technique. *Soil Dynamics and Earthquake Engineering* **97**: 289-303. 10.1016/j.soildyn.2017.02.011.

Ryden, N. and C. B. Park (2006). Fast simulated annealing inversion of surface waves on pavement using phase-velocity spectra. *Geophysics* **71**(4): R49-R58.

Song, X., H. Gu, L. Tang, S. Zhao, X. Zhang, L. Li and J. Huang (2015). Application of artificial bee colony algorithm on surface wave data. *Computers & Geosciences* **83**: 219-230. <https://doi.org/10.1016/j.cageo.2015.07.010>.

Thomson, W. T. (1950). Transmission of Elastic Waves through a Stratified Solid Medium. *Journal of Applied Physics* **21**(2): 89-93. 10.1063/1.1699629.

Wathelet, M., D. Jongmans and M. Ohrnberger (2004). Surface-wave inversion using a direct search algorithm and its application to ambient vibration measurements. *Near Surface Geophysics* **2**(4): 211-221. <https://doi.org/10.3997/1873-0604.2004018>.

Xia, J., R. D. Miller and C. B. Park (1999). Estimation of near-surface shear-wave velocity by inversion of Rayleigh waves. *Geophysics* **64**(3): 691-700.